A spin quantum bit with ferromagnetic contacts for circuit QED (EPAPS)

Audrey Cottet and Takis Kontos

Laboratoire Pierre Aigrain, Ecole Normale Supérieure,

CNRS (UMR 8551), Université P. et M. Curie,

Université D. Diderot, 24 rue Lhomond, 75231 Paris Cedex 05, France

* *To whom correspondence should be addressed : cottet@lpa.ens.fr*

(Dated: June 1, 2010)

Effective exchange fields

In this letter, we consider quantum dots subject to an effective Zeeman splitting $2\delta = 32$ μeV which is due to the hybridization of the dot orbitals with the first atomic layers of the FI contacts, or more macroscopically, to the spin-dependent confinement of electrons in the dots[1]. A splitting $2\delta = 250$ μeV has been observed in Ref.2. There exists various way to adjust the amplitude of δ. One can e.g. vary the composition of the FI material. It is also possible to change the dot size[3], or the active dot orbital. This will be illustrated below for a SWNT-based quantum dot, but we expect a similar behavior with other kinds of quantum dots.

In principle, a second type of effective Zeeman splitting $\delta_{\rm cot}$ can occur when the tunnel rate Γ_σ of electrons through the FI layers is sufficiently strong to allow cotunneling processes between the quantum dot orbitals and the itinerant states of the normal reservoirs[4,5]. Cotunneling leads (on average) to a spin-dependent renormalization of the orbital levels, responsible for $\delta_{\rm cot}$. Although the field δ was dominant in Ref. 2, δ and $\delta_{\rm cot}$ were observed simultaneously in Ref. 6, due to a larger Γ_σ. We have chosen to use a very small Γ_σ to minimize $\delta_{\rm cot}$ and base our setup on the δ splitting only, because cotunneling processes leading to $\delta_{\rm cot}$ are also responsible for decoherence effects[7]. Moreover, the splitting $\delta_{\rm cot}$ has a strong gate dependence (on an energy scale corresponding typically to the Coulomb charging energies), which would risk to enhance charge-noise induced dephasing. In our setup, the only use of the normal metal contacts is to allow a control of the double-dot occupation number. The rate Γ_σ can thus be arbitrarily small.

Electrostatic description of our setup

We assume that the central conductor of the superconducting waveguide cavity has similar capacitive couplings $\widetilde{C}_{ac}$ to the two dots. The DC gates have capacitances C_g^L and C_g^R and the normal reservoirs/FI/dot contacts have capacitances $C_{L(R)}$. The junction between the two dots has a capacitance C_m. The energy shift D varies linearly with V_{ac}, V_g^L and V_g^R. We obtain

$$\partial D/\partial V_{ac} = e\widetilde{C}_{ac}(C_R - C_L + C_g^R - C_g^L)/(C_\Sigma^L C_\Sigma^R - C_m^2) \qquad (1)$$

with $C_\Sigma^{L(R)} = C_{L(R)} + C_g^{L(R)} + C_m + \widetilde{C}_{ac}$. A coupling of the spin qubit to the electric field of the superconducting cavity is possible if $\partial D/\partial V_{ac} \neq 0$. From the above equation, this requires either $C_L \neq C_R$ or $C_g^L \neq C_g^R$, which can be obtained with a proper device fabrication. The

sensitivity of the device to charge noise depends on $\partial\nu_{01}/\partial D$ and on

$$\partial D/\partial n_g^{L(R)} = \alpha_{L(R)} e^2 (\widetilde{C}_{ac} + C_{R(L)} + C_g^{R(L)})/2(C_\Sigma^L C_\Sigma^R - C_m^2) \quad (2)$$

with $\alpha_L = 1$ and $\alpha_R = -1$. In this letter, we evaluate the performances of our setup for realistic capacitances $C_L = 50$ aF, $C_R = 5$ aF, $\widetilde{C}_{ac} = 8$ aF, $C_m = 10$ aF, and $C_g^L = C_g^R = 1$ aF. This gives $\partial D/\partial n_g^L \sim 0.7$ meV and $\partial D/\partial n_g^R \sim -3$ meV. It is thus important to use working points leading to a low $\partial\nu_{01}/\partial D$. We obtain $h\partial\nu_{01}/\partial D = 2\ 10^{-2}$ and $h\partial\nu_{01}/\partial D = 3\ 10^{-5}$ at the ON and OFF points defined in the main text. Note that in the yellow triangle of Fig.2.a of the main text, the singly occupied levels $|\emptyset,\uparrow_R\rangle$,$|\emptyset,\downarrow_R\rangle$,$|\uparrow_L,\emptyset\rangle$ and $|\downarrow_L,\emptyset\rangle$ are energetically below $|\emptyset,\emptyset\rangle$, and the doubly occupied levels $|\uparrow_L,\uparrow_R\rangle$,$|\downarrow_L,\downarrow_R\rangle$,$|\uparrow_L,\downarrow_R\rangle$ and $|\downarrow_L,\uparrow_R\rangle$. We have chosen the ON and OFF points along the dashed line $n_g^R = 0.5+(C_\Sigma^R+C_m)/(C_\Sigma^L+C_m)(0.5-n_g^L)$ in order to maximize this energy separation to a value of the order of E_c^m and $0.7E_c^m$ at the ON and OFF point respectively, with $E_c^m = C_m e^2/2(C_\Sigma^L C_\Sigma^R - C_m^2) = 0.5$ meV the mutual charging energy of the two dots. In these conditions, using very small tunnel rates through the FIs ($\Gamma_\sigma \lesssim 0.01\mu eV$) protects our setup from cotunneling-induced decoherence.

Calculation of the contact-induced spin splittings from $\hat{H}_W$

For clarity, we present the calculation for dot L only. Periodic boundary conditions along the SWNT circumference impose lowest transverse wavevectors $\varkappa_K = \varkappa_0$ and $\varkappa_{K'} = -\varkappa_0$,with $\varkappa_0 = -\nu/3R$, for pure K and K' modes. We consider a semiconducting SWNT, so that we have $\nu = \pm 1$ depending on the SWNT chiral vector. In the absence of the confinement potential $E_{pot}(\xi)$ of Eq. (2), the (spin-degenerate) eigenenergies of $\hat{H}_W$ write $E_{\eta,\mu,k} = \eta\hbar v_F\sqrt{k^2+\varkappa_0^2} + \mu\Delta_{K-K'} - E_g$, with k the longitudinal electronic wavevector. We use $\eta = \pm 1$ for the SWNT conduction and valence bands. The index $\mu = \pm 1$ is related to the K/K' degree of freedom. For a constant μ, the SWNT energy band presents a gap $\Delta_{SWNT} = 2\hbar v_F/3R = 350$ meV for $R = 1$ nm. In the presence of $E_{pot}(\xi)$, one can look for eigenvectors of $\hat{H}_W$ with the form

$$\Psi_{\eta,\mu,k}(\xi,\varphi) = A\left[\ \mu Z_{\eta_{FI1},-ik_{FI1}} e^{i\varkappa_0 R\varphi},\quad \mu e^{i\varkappa_0 R\varphi},\quad Z_{\eta_{FI1},-ik_{FI1}} e^{-i\varkappa_0 R\varphi},\quad e^{-i\varkappa_0 R\varphi}\ \right]^t e^{k_{FI1}\xi} \quad (3)$$

for $\xi < 0$,

$$\Psi_{\eta,\mu,k}(\xi,\varphi) = C \left[\mu Z_{\eta,k} e^{i\varkappa_0 R\varphi}, \quad \mu e^{i\varkappa_0 R\varphi}, \quad Z_{\eta,k} e^{-i\varkappa_0 R\varphi}, \quad e^{-i\varkappa_0 R\varphi} \right]^t e^{ik\xi} \tag{4}$$

$$+ D \left[\mu Z_{\eta,-k} e^{i\varkappa_0 R\varphi}, \quad \mu e^{i\varkappa_0 R\varphi}, \quad Z_{\eta,-k} e^{-i\varkappa_0 R\varphi}, \quad e^{-i\varkappa_0 R\varphi} \right]^t e^{-ik\xi} \tag{5}$$

for $0 < \xi < \lambda$, and

$$\Psi_{\eta,\mu,k}(\xi,\varphi) = B \left[\mu Z_{\eta_{Is},ik_{Is}} e^{i\varkappa_0 R\varphi}, \quad \mu e^{i\varkappa_0 R\varphi}, \quad Z_{\eta_{Is},ik_{Is}} e^{-i\varkappa_0 R\varphi}, \quad e^{-i\varkappa_0 R\varphi} \right]^t e^{k_{Is}(\lambda-\xi)} \tag{6}$$

for $\xi > \lambda$, with

$$Z_{\eta,k} = \eta(\varkappa_0 - ik)/\sqrt{\varkappa_0^2 + k^2} \tag{7}$$

The four components in the above vectors correspond to the (A,K), (B,K), (A,K'), and (B,K') components respectively. The potential drop at the edges of the dot is likely to occur on a length scale much larger than the SWNT lattice constant. In these conditions, the index μ is conserved along the ξ axis[8,9]. The wavevectors k_{FI1} and k_{Is} of the evanescent waves at the $FI1$ and Is sides and the factors η_{Is} and η_{FI1} depend on the wavevector k, the valence/conduction index η and the spin σ of the electron confined in dot L. They can be obtained from

$$E = \eta\hbar v_F \sqrt{k^2 + \varkappa_0^2} + \mu\Delta_{K-K'} + E_g^L \tag{8}$$

$$= \eta_{FI1}\hbar v_F \sqrt{\varkappa_0^2 - k_{FI1}^2} + \mu\Delta_{K-K'} - \sigma E_{ex}/2 + E_b \tag{9}$$

$$= \eta_{Is}\hbar v_F \sqrt{\varkappa_0^2 - k_{Is}^2} + \mu\Delta_{K-K'} + E_{Is} \tag{10}$$

The continuity of $\Psi_{n,\mu,k}$ at $\xi = 0$ and $\xi = \lambda$ imposes a longitudinal quantization condition

$$e^{2ik\lambda} = \frac{(Z_{\eta,k} - Z_{\eta_{FI1},-ik_{FI1}})\,(Z_{\eta,-k} - Z_{\eta_{FI1},ik_{Is}})}{(Z_{\eta,-k} - Z_{\eta_{FI1},-ik_{FI1}})\,(Z_{\eta,k} - Z_{\eta_{FI1},ik_{Is}})} \tag{11}$$

We note n the mode index related to the longitudinal confinement of electrons. Apart from the solution $k_{n=0}^{\sigma}(E) = 0$, all the solutions $k = k_n^{\sigma}(E)$ depend on spin due to $E_{ex} \neq 0$, but are independent of μ. This leads to an effective spin-splitting $2\delta_L$ inside dot L, which depends on n but not on μ. Here, we use $R = 1$ nm, $\lambda = 100$ nm and $E_{ex} = 3.7$ meV. A numerical resolution of Eq. (11) gives the values of δ_L shown in Fig. 1 of the EPAPS. Due to the existence of the SWNT bandgap, we obtain a sweet spot $\partial\delta^L/\partial E_g^L = 0$ which can be used to reduce charge noise-induced dephasing mediated by fluctuations of δ^L. We find that the

value of δ_L at the sweet spot increases with n and decreases with λ. This provides interesting means to adjust the value of δ_L, independently of the FI/SWNT contact properties. In the main text, we assume $\Delta_{K-K'} > 0$ and define the $|\uparrow_L, \emptyset\rangle$ and $|\downarrow_L, \emptyset\rangle$ states as the 29^{th} lowest pair of spin-dependent levels in the dot conduction band, i.e. $\eta = +1$, $n = 15$ and $\mu = -1$, but other choices are possible, depending on the value of E_{ex}. We have checked that the spin-orbit coupling term $\Delta^{\parallel}_{curv}$ introduced in Ref. 9 slightly renormalizes $\Delta_{K-K'}$, but does not affect the principle of our setup and the value of δ_L. Note that the longitudinal quantization of electrons corresponds to an intrinsic level spacing $\Delta E \sim hv_F/2\lambda = 16.5$ meV, and one has typically $\Delta_{K-K'} = 3$ meV[10,11]. Hence, the levels $|\uparrow_L, \emptyset\rangle$ and $|\downarrow_L, \emptyset\rangle$ are sufficiently far from other orbitals of dot L to allow the qubit operation described in the main text (similar considerations can be done for dot R).

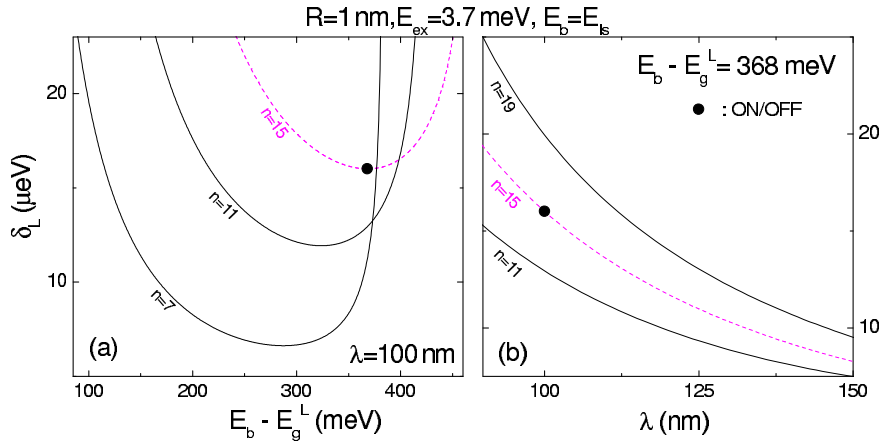

FIG. 1: Half effective Zeeman splitting δ^L calculated for dot L in the framework of Eq.(2) of the main text, as a function of $E_b - E_g^L$ (panel a) and the nanotube length λ (panel b). We have used various values for the orbital index n, $\eta = +1$, $R = 1$ nm, $\lambda = 100$ nm, $E_b = E_{Is}$ and $E_{ex} = 3.7$ meV. We indicate the position of the ON/OFF points considered in the main text.

Dephasing caused by charge noise

In practice, the dots L and R will be affected by low frequency charge noise, like all Coulomb blockade devices. This noise is generally attributed to two level charge fluctuators located e.g. in the substrate of the sample. Although 1/f noise is frequently observed in quantum dots, few quantitative data are available in the low temperature regime. Here, we focus on the case of SWNT-based quantum dots. We assume that the charge fluctuators

lead to a typical 1/f noise spectrum

$$S_{n_g^{L(R)}}(f) = A^2/|f| \tag{12}$$

on each gate, with the definition $S_{n_g^{L(R)}}(f) = 2\int_{-\infty}^{+\infty} n_g^{L(R)}(t) n_g^{L(R)}(t+\tau)\exp(i2\pi f\tau)$. We expect a lower charge noise than in standard metallic systems[12] due to the smaller size of the devices. From Ref. 13, for a quantum dot with length $\lambda = 500$ nm, one can estimate $A = 5.4\ 10^{-4}$ at $T = 1.5$ K. It has been checked experimentally that $S_{n_g^{L(R)}}$ is proportional to λ[14]. We also assume that $S_{n_g^{L(R)}}$ scales with T^2 down to low temperatures, as observed for superconducting circuits on Si substrates[15,16]. This gives $A = 3\ 10^{-6}$ for parameters compatible with our proposal i.e. $\lambda = 100$ nm and $T = 20$ mK. We first assume that the dot gates are subject to independent fluctuations with a similar spectrum. The dephasing rate can be estimated in a semi-classical approach as[17–19]

$$T_\varphi^D = \left[2\pi A \left|\frac{\partial \nu_{01}}{\partial D}\right| \left(\left|\frac{\partial D}{\partial n_g^R}\right| + \left|\frac{\partial D}{\partial n_g^L}\right|\right)\right]^{-1} \tag{13}$$

i.e. $T_\varphi^D = 2.9$ μs at the ON point and $T_\varphi^D = 1.9$ ms at the OFF point with the parameters used in the main text. These values are probably underestimated because charge fluctuations seen by n_g^R and n_g^L should be correlated, at least partially, due to the small size of the device[12]. Assuming a perfect correlation between n_g^R and n_g^L, we obtain

$$T_\varphi^D = \left[2\pi A \left|\frac{\partial \nu_{01}}{\partial D}\right| \left(\left|\frac{\partial D}{\partial n_g^R} + \frac{\partial D}{\partial n_g^L}\right|\right)\right]^{-1} \tag{14}$$

i.e. $T_\varphi^D = 4.6$ μs at the ON point and $T_\varphi^D = 3.1$ ms at the OFF point. The dephasing time is longer in this case because $\partial D/\partial n_g^L$ and $\partial D/\partial n_g^R$ have opposite signs (see Eq. (2)). In the main text, we use the pessimistic estimate of T_φ^D given by Eq. (13). Interestingly, using suspended SWNTs (or nanowires) should allow to decrease the charge noise amplitude A and thus T_φ^D (see Ref. 20).

Dephasing mediated by δ_L fluctuations

>From the expression of $\hat{H}$, one can check that the amplitude of ν_{01} corresponds mainly to $2\delta_L$ for $D > \delta_L + \delta_R + t$. Since δ_L depends on E_g^L, this opens a new path to charge noise dephasing (the δ_R-path can be disregarded since $\partial\nu_{01}/\partial\delta_R \ll \partial\nu_{01}/\partial\delta_L$). We work at the sweet spot $\partial\delta_L/\partial E_g^L = 0$ of Fig.4. We assume that n_g^L and n_g^R are subject to independent fluctuations with a similar spectrum (see Eq. (12) of the EPAPS). Considering second order contributions of the charge noise to δ_L in a semi-classical approach[18,19,21], we obtain

$$T_{\varphi}^{\delta_L} \sim \left[2\pi A^2 \left| \frac{\partial \nu_{01}}{\partial \delta_L} \frac{\partial^2 \delta_L}{\partial (E_g^L)^2} \right| \left(\left| \frac{\partial E_g^L}{\partial n_g^L} \right|^2 + \left| \frac{\partial E_g^L}{\partial n_g^R} \right|^2 \right) \right]^{-1} \tag{15}$$

Using $\partial E_g^L/\partial n_g^L = -C_\Sigma^R e^2/(C_\Sigma^L C_\Sigma^R - C_m^2)$ and $\partial E_g^L/\partial n_g^R = -C_m e^2/(C_\Sigma^L C_\Sigma^R - C_m^2)$, we obtain $T_{\varphi}^{\delta_L} \sim 15$ ms at the ON and OFF points with the parameters used in the main text.

Relaxation caused by phonons

Since the $|\mathbf{0}\rangle$ and $|\mathbf{1}\rangle$ states have slight components in $\downarrow_L$ and $\uparrow_L$ respectively, they can relax due to electron/phonon interaction. In SWNTs, phonons modes can be classically described with a continuous atomic displacement $u_{m,q}(\xi,\varphi) = A\exp(i(m\varphi + q\xi - \omega t))$, with A a vector in the (φ,ξ,r) cylindrical frame of the SWNT. From Eqs.(3-6) of the EPAPS and the form of the electron-phonon interaction[22], one can check that the only modes which can induce transitions between the $|\mathbf{0}\rangle$ and $|\mathbf{1}\rangle$ states are those with $m = 0$. We take into account the acoustic mode most strongly coupled to the SWNT electrons, i.e. the stretching mode[22]. In the limit $qR \ll 1$, this mode has a dispersion relation $\omega_S = c_S\,|q|$, and a displacement vector $u_{0,q}^S(\xi,\varphi) \propto (0,1,-iqR\eta)\exp(i(q\xi - \omega t))$ with $\eta = 1 - 2(c_l^2/c_t^2) \simeq 0.3$, $c_t = 12.3$ km.s^{-1}, $c_l = 21$ km.s^{-1} and $c_S = 20$ km.s^{-1}. Remarkably, the contacts evaporated on top of SWNTs confine phonons efficiently, as shown by the observation of quantized modes called "vibrons" in suspended SWNTs[23–25]. This should remain true for non-suspended structures, for which the contacts are similar. We thus consider decoupled stretching vibrons for the left and right dots. Assuming that the phonons are quickly damped below the Is, $FI1$ and $FI2$ gates, one finds that the stretching vibrons of dot L and R have displacement vectors proportional to $(0, \sin(q_p\xi), -iqR\eta\cos(q_p\xi))$ with $0 \le \xi \le L$ and to $(0, \sin(q_p(\xi - a)), -iqR\eta\cos(q_p(\xi - a)))$ with $a \le \xi \le a + L$ respectively, with $q_p = p\pi/\lambda$, $p \in \mathbb{N}$. For nanotube sections with length $\lambda = 100$ nm, these vibrons occur at frequencies $\nu_{ph,p} = p * 100$ GHz which are much larger than the qubit transition frequency $\nu_{01} = 7.68$ GHz. In non-suspended structures, low energy vibrons are usually not observed, which indicates that they are damped due to the contact with the substrate. This can be described in a phenomenological approach by considering that the vibrons have a lifetime Γ^{-1}, with Γ comparable to $\hbar\nu_{ph,1}$. In this framework, the relaxation time of the qubit due to the vibrons can be estimated as

$$T_1^{-1} = \sum_{\substack{l\in\{L,R\} \\ p\in\mathbb{N}}} \hbar\tilde{g}_{l,p}^2 \frac{\Gamma}{\left(\frac{\Gamma}{2}\right)^2 + (h\nu_{ph,p} - h\nu_{01})^2} \tag{16}$$

by analogy with the Purcell effect[26]. We have introduced above the coupling constant $\tilde{g}_{l,p}$ between the qubit and the p^{th} vibron mode of dot $l \in \{L, R\}$. One can use the above formula provided $\hbar\tilde{g}_{l,p} \ll \Gamma$. In order to calculate $\tilde{g}_{l,p}$, we decompose the $|\mathbf{0}\rangle$ and $|\mathbf{1}\rangle$ states as

$$|\mathbf{0/1}\rangle = \alpha^{0/1}_{\uparrow_L} |\uparrow_L, \emptyset\rangle + \alpha^{0/1}_{\downarrow_L} |\downarrow_L, \emptyset\rangle + \alpha^{0/1}_{\uparrow_R} |\emptyset, \uparrow_R\rangle + \alpha^{0/1}_{\downarrow_R} |\emptyset, \downarrow_R\rangle \tag{17}$$

The weights $\alpha^{0/1}_{\uparrow(\downarrow)_{L[R]}}$ can be calculated from Eq.(1) of the main text. The coupling of electrons to the p^{th} vibron mode of dot l can be described by adding to $\hat{H}_{SWNT}$ an electron-vibron interaction term

$$H^{l,p}_{ph}(\xi) = M_{l,p}\left(b_q + b^\dagger_q\right) \tag{18}$$

with[27]

$$M_{L,p}(\xi) = 2\sqrt{2}\mathcal{C}_1\left(c_t^2/c_l^2\right) q_p \cos(q_p\xi)\hat{s}_0\hat{\gamma}_0\theta[\xi]\theta[\lambda - \xi]\mathcal{N} \tag{19}$$

$$M_{R,p}(\xi) = 2\sqrt{2}\mathcal{C}_1\left(c_t^2/c_l^2\right) q_p \cos(q_p(\xi - \lambda - a))\hat{s}_0\hat{\gamma}_0\theta[\xi - \lambda - a]\theta[\lambda - 2\xi - a]\mathcal{N} \tag{20}$$

and

$$\mathcal{N} = \sqrt{\hbar/4\pi M_\lambda \nu_{ph,p}} \tag{21}$$

We use $\mathcal{C}_1 \simeq 30$ eV, while $\theta[\xi]$ is Heavidside function. The mass M_λ of a SWNT section with length λ can be calculated as $M_\lambda = 8\pi M_C R\lambda/3\sqrt{3}a_0^2$, with $a_0 = 0.142$ nm and M_C the atomic mass of carbon. We disregard the $\hat{s}_{1(2)}\hat{\gamma}_{0(3)}$ components of $M_{L(R),p}(\xi)$ because they occur together with a constant $\mathcal{C}_2 \simeq 1.5$ eV $\ll\mathcal{C}_1$[22]. We finally obtain

$$\hbar\tilde{g}_{L,p} = \left|\left(\alpha^1_{\uparrow_L}\right)^* \alpha^0_{\uparrow_L} \langle\uparrow_L, \emptyset| M_{L,p} |\uparrow_L, \emptyset\rangle + \left(\alpha^1_{\downarrow_L}\right)^* \alpha^0_{\downarrow_L} \langle\downarrow_L, \emptyset| M_{L,p} |\downarrow_L, \emptyset\rangle\right| \tag{22}$$

and

$$\hbar\tilde{g}_{R,p} = \left|\left(\alpha^1_{\uparrow_R}\right)^* \alpha^0_{\uparrow_R} \langle\emptyset, \uparrow_R| M_{R,p} |\emptyset, \uparrow_R\rangle + \left(\alpha^1_{\downarrow_R}\right)^* \alpha^0_{\downarrow_R} \langle\emptyset, \downarrow_R| M_{R,p} |\emptyset, \downarrow_R\rangle\right| \tag{23}$$

We recall that the wavefunctions corresponding to $|\uparrow(\downarrow)_L, \emptyset\rangle$ and $|\emptyset, \uparrow(\downarrow)_R\rangle$ can be obtained from Eqs. (3-6), and (11) of the EPAPS. For $Q_{ph} = h\nu_{ph,1}/\Gamma = 1.5$, we obtain relaxation times $T_1^{ON} = 1.0$ μs and $T_1^{OFF} = 0.21$ s at the ON and OFF points respectively. Remarkably, with a suspended SWNT, Γ should be strongly reduced and T_1 should be enhanced thanks to a Purcell-like effect. For instance, with $Q_{ph} = 20$, we obtain $T_1^{ON} \simeq 14$ μs and $T_1^{OFF} \simeq 2.8$ s.

---

[1] A. Cottet and M.-S. Choi, Phys. Rev. B **74**, 235316 (2006).

[2] S. Sahoo, T. Kontos, J. Furer et al. Nature Phys. **1**, 99 (2005).

[3] A. Cottet, T. Kontos, W. Belzig, C. Schönenberger, C. Bruder, Europhys. Lett. **74**, 320 (2006).

[4] J. Martinek, Y. Utsumi, H. Imamura et al., Phys. Rev. Lett. **91**, 127203 (2003).

[5] M. Braun, J. König and J. Martinek, Phys. Rev. B **70**, 195345 (2004).

[6] J.R. Hauptmann, J. Paaske, P. E. Lindelof, Nature Phys. **4**, 373 (2008).

[7] B. Dong, N.J.M. Horing, H.L. Cui, Phys. Rev. B **72**, 165326 (2005).

[8] D.P. DiVincenzo and E.J. Mele, Phys. Rev. B **29**, 1685 (1983).

[9] D. V. Bulaev, B. Trauzettel and D. Loss, Phys. Rev. B **77**, 235301 (2008).

[10] W. Liang,M. Bockrath, H. Park, Phys. Rev. Lett. **88**, 126801 (2002).

[11] S. Sapmaz, P. Jarillo-Herrero, J. Kong et al., Phys. Rev. B **71**, 153402 (2005).

[12] A.B. Zorin, F.-J. Ahlers, J. Niemeyer, T. Weimann, H. Wolf, V.A. Krupenin, and S. V. Lotkhov, Phys. Rev. B **53**, 13682 (1995).

[13] L.G. Herrmann, T. Delattre et al. Phys. Rev. Lett. **99**, 156804 (2007).

[14] J. Männik, I. Heller, A.M. Janssens, S.G. Lemay, and C. Dekker Nano Lett. **8**, 685 (2008).

[15] O. Astafiev, Yu. A. Pashkin, Y. Nakamura, T. Yamamoto and J.S. Tsai, Phys. Rev. Lett. **96**, 137001 (2006).

[16] F.C. Wellstood, C. Urbina, and J. Clarke, Appl. Phys. Lett. **85**, 5296 (2004).

[17] A. Cottet, A. Steinbach, P. Joyez, D. Vion, H. Pothier, D. Esteve and M.E. Huber in: "Macroscopic Quantum Coherence and Quantum Computing", edited by D.V. Averin, B. Ruggiero, P. Silvestrini (Kluwer Academic, Plenum Publishers, New York , 2001).

[18] J. Koch et al. *Phys. Rev. A* **76**, 042319 (2007).

[19] Y. Makhlin and A. Schnirman Phys. Rev. Lett. **92**, 178301 (2004)

[20] Roschier, L.R. Tarkiainen, M. Ahlskog, M. Paalanen and P. Hakonen, Appl. Phys. Lett. **78**, 3295 (2001).

[21] G. Ithier, E. Collin, P. Joyez et al., Phys. Rev. B **72**, 134519 (2005).

[22] H. Suzuura and T. Ando, Phys. Rev. B **65**, 235412 (2002).

[23] S. Sapmaz, P. Jarillo-Herrero, Ya. M. Blanter, Phys. Rev. Lett. **96**, 026801 (2006).

[24] A.K. Huttel, B. Witkamp, M. Leijnse, M.R. Wegewijs, and H.S.J. van der Zant, Phys. Rev. Lett. **102**, 225501 (2009).

[25] R. Leturcq, C. Stampfer, K. Inderbitzin et al. Nature Phys. **5**, 327 (2009).

[26] D.Kleppner, Phys. Rev. Lett. **47**, 233 (1981).

[27] E. Mariani and F. Von Oppen, Phys. Rev. B **80**, 155411 (2009).